Hindawi
Mathematical Problems in Engineering
Volume 2020, Article ID 6750369, 7 pages
https://doi.org/10.1155/2020/6750369

Research Article

An Anisotropic Hyperelastic Constitutive Model with Bending Stiffness Interaction for Cord-Rubber Composites: Comparison of Simulation Results with Experimental Data

Shulei Sun [1] and Wenguo Chen [2]

[1] *Department of Mechanics Engineering, Guizhou Institute of Technology, Guiyang 550003, China*
[2] *School of Information Engineering, Qujing Normal University, Quijing 655011, China*

Correspondence should be addressed to Shulei Sun; 932846297@qq.com

Received 10 March 2020; Revised 14 June 2020; Accepted 30 June 2020; Published 24 July 2020

Academic Editor: A. M. Bastos Pereira

Based on the invariant theory of continuum mechanics by Spencer, the strain energy depends on deformation, fiber direction, and the gradients of the fiber direction in the deformed configuration. The resulting extended theory is very complicated and brings a nonsymmetric stress and couple stress. By introducing the gradient of fiber vector in the current configuration, the strain energy function can be decomposed into volumetric, isochoric, anisotropic, and bending deformation energy. Due to the particularity of bending deformation, the reinforced material has tensile deformation and compression deformation. The bending stiffness should be taken into consideration, and it is further verified by the bending simulation.

1. Introduction

The theory of finite deformation of fiber-reinforced composites based on the continuum mechanics theory was first proposed and established by Adkins and Rivlin [1]. Spencer used the invariant method [2, 3] to represent the fiber direction as a unit vector in the reference configuration. Spencer further refined the theory of finite deformation of fiber-reinforced composites. This method is widely used in the finite deformation of composite materials, especially in the industrial and biomechanical fields, i.e., air compression springs composed of fiber-reinforced materials [4] and intervertebral disc tissue in biology, and it achieved success. The results demonstrate the effectiveness of this model. Peng et al. proposed a new constitutive equation [5], which divides the energy function (per unit reference volume) of human intervertebral disc annulus into three parts: matrix, fiber, and the interaction of the two, and determines the material parameters, experiments, and simulation through step by step experiments. The data are in good agreement. Another important application in biomechanics is the establishment of arterial wall constitutive [6]. Steigmann developed a model for the mechanics of woven fabrics in the framework of two-dimensional elastic surface theory [7]. The implementation of an enhanced modelling approach for fiber-reinforced composites is presented which may, in addition to the directional dependency induced by the fibers, allow the capturing of the fiber bending stiffness [8]. Comparison of simulation results with analytical solutions was made with respect to the fiber-reinforced composites with fiber bending stiffness under azimuthal shear [9]. Soldatos researched the invention of methods appropriate for characterization of fiber-reinforced materials that exhibit polar material behavior due to fiber bending resistance [10]. A linear model, framed in the setting of the second strain gradient theory, is presented for the mechanics of an elastic solid reinforced with fibers resistant to flexure [11].

However, when this homogenous constitutive model based on continuum mechanics is applied to the bending model, it is found that the constitutive model cannot accurately describe the mechanical behavior of bending [3]. There is a premise that the fiber is infinitely soft under uniaxial compressive condition. This is a valid assumption in most cases, such as stretching and compression. In the conventional theory, there are no parameters in terms of dimensions, and thus it cannot explain the size effect in any aspect. For this reason, Spencer established an invariant-based model that considers the fiber size effect [3], but the model is too complex for practical application.

Based on the invariant theory established by Spencer [12], this paper attempts to establish an anisotropic hyperplastic constitutive model with bending stiffness, i.e., increasing the parameter dependent on the fiber direction vector gradient in current deformation and establishing the relationship with curvature. The comparison between the simulation results and the bending experimental data of the rubber-cord composite proves the correctness of the model.

2. Rubber-Cord Constitutive Model

2.1. Constitutive Model of Conventional Anisotropic Hyperelastic Fiber-Reinforced Composites. According to Spencer's theory of anisotropic fiber-reinforced composites [3], the Helmholtz strain energy function (per unit reference volume) **W** depends on the deformation and fiber direction a_0:

$$W = W(C, A), \tag{1}$$

where the tensor **F** is deformation gradient t, the tensor $C = F^T \cdot F$ is the right Cauchy–Green deformation, and the tensor **A** $(a_0 \otimes a_0)$ is of order two.

The Helmholtz strain energy function per unit volume **W** can also be written in the form of invariants for **C** and **A**:

$$\begin{aligned} W &= W\left[I_1(C), I_2(C), I_3(C), I_4(C, A), I_5(C, A)\right], \\ I_1(C) &= \operatorname{tr}(C), \\ I_2(C) &= \frac{1}{2}\left[\left(\operatorname{tr}(C)^2 - \operatorname{tr}\left(C^2\right)\right)\right], \\ I_3(C) &= \det(C), \\ I_4 &= (C, A) = A \cdot C \cdot A, \\ I_5(C, A) &= A \cdot C^2 \cdot A. \end{aligned} \tag{2}$$

Since the deformation gradient **F** can be decomposed into volume-preserving deformation and volumetric deformation, the strain energy function **W** may be expressed as a function of the following three parts [6]:

$$W = W_{\text{vol}}(J) + W_{\text{iso}}\left(\overline{I}_1, \overline{I}_2\right) + W_{\text{ani}}\left(\overline{I}_4, \overline{I}_5\right), \tag{3}$$

where W_{vol}, W_{iso}, and W_{ani} denote the elastic deformation energy caused by volume deformation, isotropic deformation, and anisotropic deformation, respectively.

$J - \sqrt{I_3} = \det(\mathbf{F})$ is the deformation volume ratio, and $\overline{I}_1$, $\overline{I}_2$, $\overline{I}_4$, and $\overline{I}_5$ are the corresponding partial invariants:

$$\begin{aligned} \overline{I}_1 &= J^{(-2/3)} I_1, \\ \overline{I}_2 &= J^{(-4/3)} I_2, \\ \overline{I}_4 &= J^{(-2/3)} I_4, \\ \overline{I}_5 &= J^{(-4/3)} I_5. \end{aligned} \tag{4}$$

In order to facilitate parameter fitting, the strain energy can also be given by

$$W = W_F + W_M + W_{FM}, \tag{5}$$

where W_M equivalent to W_M formula (3) $W_{\text{vol}} + W_{\text{iso}}$, $W_F + W_{FM}$ equivalent to W_{ani} formula (3) W_{ani}. According to the above analysis, for anisotropic fiber-reinforced composites that consider compressibility, a common form of strain energy per unit volume has the form [8–10]

$$\begin{aligned} W = {} & \frac{1}{D}(J-1)^2 + \sum_{i=1}^{3} a_i\left(\overline{I}_1 - 3\right)^i + \sum_{j=1}^{3} b_i\left(\overline{I}_2 - 3\right)^j + \sum_{k=2}^{6} c_i\left(\overline{I}_4 - 1\right)^k \\ & + \sum_{l=1}^{6} d_i\left(\overline{I}_5 - 1\right)^1. \end{aligned} \tag{6}$$

By means of chain rule, the second-order Piola–Kirchhoff stress tensor can be obtained by deriving the strain energy function with respect to the right Cauchy–Green variable **C**. We write

$$\mathbf{S} = \mathbf{S}_{\text{vol}} + \mathbf{S}_{\text{iso}} + \mathbf{S}_{\text{ani}} = 2\frac{\partial \mathbf{W}}{\partial \mathbf{C}}. \tag{7}$$

In particular, we consider the incompressible materials and obtain the form

$$\mathbf{S}_{\text{iso}} + \mathbf{S}_{\text{ani}} = J^{(-2/3)} Dev\left(2\sum_{\substack{\alpha-1 \\ \alpha \neq 3}}^{5} \frac{\partial W_{\text{iso+ani}}}{\partial \overline{I}_\alpha} \frac{\partial \overline{I}_\alpha}{\partial \overline{\mathbf{C}}}\right), \tag{8}$$

where $Dec(\cdot) = (\cdot) - (1/3)[(\cdot)\colon \mathbf{C}]\mathbf{C}^{-1}$.

$$\begin{aligned} \frac{\partial \overline{I}_1}{\partial \overline{\mathbf{C}}} &= \mathbf{I}, \\ \frac{\partial \overline{I}_2}{\partial \overline{\mathbf{C}}} &= \overline{I}_1 \mathbf{I} - \overline{\mathbf{C}}, \\ \frac{\partial \overline{I}_4}{\partial \overline{\mathbf{C}}} &= \mathbf{A} \otimes \mathbf{A}, \\ \frac{\partial \overline{I}_5}{\partial \overline{\mathbf{C}}} &= \mathbf{A} \otimes \overline{\mathbf{C}} \cdot \mathbf{A} + \mathbf{A} \cdot \overline{\mathbf{C}} \otimes \mathbf{A}, \\ \mathbf{S}_{\text{vol}} &= 2\frac{\partial W_{\text{vol}}}{\partial \mathbf{C}} = J p \mathbf{C}^{-1}, \end{aligned} \tag{9}$$

where $p = (\mathrm{d}W_{\text{vol}}/\mathrm{d}J)$,

The Cauchy stress tensor is defined to be

$$\boldsymbol{\sigma} = \frac{2}{J}\mathbf{F}\frac{\partial W}{\partial \mathbf{C}}\mathbf{F}^T. \tag{10}$$

2.2. Constitutive Model of Fiber-Reinforced Composites with Bending Stiffness. The form of strain energy in a conventional constitutive model depends only on both the deformation gradient $\mathbf{F}$ and the fiber direction tensor $\mathbf{A}$. For a material reinforced by a single family of fibers, the fiber direction is defined by a unit vector field $\mathbf{A}$ in the reference configuration and a unit vector field $\mathbf{a}$ in the deformed configuration. A single family of fibers here mainly refers to the direction of fiber arrangement and single means a direction for fibers. The fibers are convected with the material, and thus

$$\mathbf{F}\cdot\mathbf{A} = \lambda\mathbf{a} = \mathbf{b}. \tag{11}$$

When considering the contribution with the bending stiffness, we need to increase the fiber direction vector $\mathbf{b}$ and the tensor $\mathbf{G}$, which is given by $\mathbf{G} = \partial\mathbf{b}/\partial\mathbf{X}$. By analogy with relation (12), we may postulate the free energy per unit reference energy:

$$W = W(\mathbf{F}, \mathbf{G}, \mathbf{A}). \tag{12}$$

The free energy must be unchanged if the fiber-reinforced composite undergoes a rotation described by the proper orthogonal tensor Q. We obtain the following expressions:

$$W(\mathbf{F}, \mathbf{G}, \mathbf{A}) = W(\mathbf{Q}\cdot\mathbf{F}, \mathbf{Q}\cdot\mathbf{G}, \mathbf{A}), \tag{13}$$

where $\mathbf{Q}$ is arbitrary orthogonal tensor. The tensors $\mathbf{F}$ and $\mathbf{G}$ can be written in the form of a scalar product, respectively:

$$\begin{aligned} \mathbf{C} &= \mathbf{F}^T\cdot\mathbf{F},\\ \Gamma &= \mathbf{G}^T\cdot\mathbf{G},\\ \boldsymbol{\Lambda} &= \mathbf{F}^T\cdot\mathbf{G}. \end{aligned} \tag{14}$$

Hence, we can get $\Gamma = \Lambda^T\mathbf{C}^{-1}\Lambda$ using the Cayley–Hamilton formulation [11]:

$$I_3\mathbf{C}^{-1} = \mathbf{C}^1 - I_1\mathbf{C} + I_2\mathbf{I}. \tag{15}$$

Let the tensor Γ be represented by the invariants of Λ. Finally, the function W that can be represented as $\Lambda, \mathbf{C}, \mathbf{A}$ is expressed as

$$W = W(\boldsymbol{\Lambda}, \mathbf{C}, \mathbf{A}). \tag{16}$$

According to the formula in Zheng [12], the free energy W consists of 33 invariants (Table 1) $\Lambda, \mathbf{C}, \mathbf{A}$ about isotropic, which is too complicated. In order to simplify the constitutive equation, it is now assumed that the W curvature of the fiber is more strictly dependent, i.e., the directional derivative deformation gradient $\mathbf{A}(\partial\mathbf{b}/\partial\mathbf{X}) = \mathbf{A}\cdot\mathbf{G} = \kappa$ of the fiber direction vector $\mathbf{A}$ after deformation and the unit vector before deformation $\mathbf{F}$, i.e.,

$$W = W\left(\mathbf{F}, \mathbf{A}, \mathbf{A}\frac{\partial\mathbf{b}}{\partial\mathbf{X}}\right). \tag{17}$$

By analogy with the $\mathbf{F}$ and $\mathbf{G}$, the tensor $\mathbf{F}, \kappa$ can be written in the form of product, respectively:

$$\begin{aligned} \mathbf{C} &= \mathbf{F}^T\cdot\mathbf{F},\\ \mathbf{K} &= \kappa\mathbf{F} = \mathbf{A}\cdot\mathbf{G}\cdot\mathbf{F},\\ \kappa^2 &= \kappa\kappa. \end{aligned} \tag{18}$$

This W can be expressed as a function of $\mathbf{C}$, $\mathbf{A}, \mathbf{K}, \kappa^2$:

$$W = W\left(\mathbf{C}, \mathbf{A}, \mathbf{K}, \kappa^2\right). \tag{19}$$

According to the representation theory of the tensor function [12], a total of 11 invariants can be expressed, where the first five invariants are the same as in the formula (2).

$$\begin{aligned} I_6 &= \mathbf{K}\cdot\mathbf{K} = \mathbf{A}\cdot\boldsymbol{\Lambda}^T\cdot\boldsymbol{\Lambda}\cdot\mathbf{A},\\ I_7 &= \mathbf{K}\cdot\mathbf{C}\cdot\mathbf{K} = \mathbf{A}\cdot\boldsymbol{\Lambda}^T\cdot\mathbf{C}\cdot\boldsymbol{\Lambda}\cdot\mathbf{A},\\ I_8 &= \mathbf{K}\cdot\mathbf{C}^2\cdot\mathbf{K} = \mathbf{A}\cdot\boldsymbol{\Lambda}^T\cdot\mathbf{C}^2\cdot\boldsymbol{\Lambda}\cdot\mathbf{A},\\ \mathrm{I}_9 &= \mathbf{A}\cdot\mathbf{K} = \mathbf{A}\cdot\boldsymbol{\Lambda}\cdot\mathbf{A},\\ I_{10} &= \mathbf{A}\cdot\mathbf{C}\cdot\mathbf{K} = \mathbf{A}\cdot\mathbf{C}\cdot\boldsymbol{\Lambda}\cdot\mathbf{A},\\ I_{11} &= \mathbf{A}\cdot\mathbf{C}^2\cdot\boldsymbol{\Lambda}\cdot\mathbf{A}, \end{aligned} \tag{20}$$

where $\Lambda = \mathbf{F}\cdot\mathbf{G}$ can be obtained by equation (19). From equation (19),

$$\begin{aligned} &\frac{\partial I_6}{\partial\mathbf{C}} = 0,\\ &\frac{\partial I_7}{\partial\mathbf{C}} = (\boldsymbol{\Lambda}\cdot\mathbf{A})\otimes(\boldsymbol{\Lambda}\cdot\mathbf{A}),\\ &\frac{\partial I_8}{\partial\mathbf{C}} = \boldsymbol{\Lambda}\cdot\mathbf{A}\otimes(\mathbf{C}\cdot\boldsymbol{\Lambda}\cdot\mathbf{A}),\\ &\frac{\partial I_9}{\partial\mathbf{C}} = 0,\\ &\frac{\partial I_{10}}{\partial\mathbf{C}} = \mathbf{A}\otimes(\boldsymbol{\Lambda}\cdot\mathbf{A}),\\ &\frac{\partial I_{11}}{\partial\mathbf{C}} = \mathbf{A}\otimes(\mathbf{C}\cdot\boldsymbol{\Lambda}\cdot\mathbf{A}),\\ &\frac{\partial I_6}{\partial\boldsymbol{\Lambda}} 2\boldsymbol{\Lambda}\cdot\mathbf{A}\otimes\mathbf{A},\\ &\frac{\partial I_7}{\partial\mathbf{A}} 2(\mathbf{C}\cdot\boldsymbol{\Lambda}\cdot\mathbf{A})\otimes\mathbf{A},\\ &\frac{\partial I_7}{\partial\boldsymbol{\Lambda}} = 2\left(\mathbf{A}^2\cdot\boldsymbol{\Lambda}\cdot\mathbf{A}\right)\otimes\mathbf{A},\\ &\frac{\partial I_9}{\partial\boldsymbol{\Lambda}} = \mathbf{A}\otimes\mathbf{A},\\ &\frac{\partial I_{10}}{\partial\boldsymbol{\Lambda}} = (\mathbf{C}\cdot\mathbf{A})\otimes\mathbf{A},\\ &\frac{\partial I_{11}}{\partial\boldsymbol{\Lambda}} = \left(\mathbf{C}^2\cdot\mathbf{A}\right)\otimes\mathbf{A}. \end{aligned} \tag{21}$$

TABLE 1: Invariants in the three-dimensional isotropic and hemitropic irreducible function bases of A_i, W_P, and V_{rn} [12].

Agencies	Isotropy	Hemitropy
A		tr A, tr A^2, tr A^3
A, B		tr AB, tr A^2B, tr AB^2, tr $A^2 B^2$
A, B, C		tr ABC
W		tr W^2
A, W		tr AW^2, tr $A^2 W^2$, tr $A^2 W^2 AW$
A, B, W		tr ABW, tr $A^2 BW$, tr $AB^2 W$, tr AW^2BW
W, V		tr WV
A W, V		tr AWV, tr $AW^2 V$, tr $AW V^2$
W, V, U		tr WVU
V	$v\cdot v$	$v\cdot v$
A, v	$v\cdot Av$, $v\cdot A^2 v$	$v\cdot Av$, $v\cdot A^2 v$, $[v, Av, A^2 v]$
A, B, v	$v\cdot Abv$	$v\cdot \varepsilon\ [AB]$, $v\cdot\varepsilon[A^2B]$, $v\cdot\varepsilon\ [AB^2]$, $[, v, Av, Bv]$
W, v	$v\cdot W^2 v$	$v\cdot\varepsilon\ [W]$
A, W, v	$v\cdot Awv$, $v\cdot A^2 Wv$, $v\cdot WAW^2 v$	$v\cdot AWv$, $v\cdot\varepsilon\ [AW]$, $v\cdot\varepsilon\ [AW^2]$
W, V, v	$v\cdot WVv$, $v\cdot W^2 Vv$, $v\cdot WV^2 v$	$v\cdot\varepsilon\ [WV]$
v, u	$v\cdot u$	$v\cdot u$
A, v, u	$v\cdot Au$, $v\cdot A^2u$	$v\cdot Au$, $[v, u, Av]$, $[v, u, Au]$
A, B, v, u	$v\cdot(AB-BA)\ u$	
W, v, u	$v\cdot Wu$, $v\cdot W^2 u$	$v\cdot Wu$
A, W, v, u	$v\cdot(AW+WA)\ u$	
W, V, v, u	$v\cdot(WV-VW)\ u$	
v, u, w		$[v, u, w]$

In summary, the total strain energy with the bending stiffness is in the form of

$$W = W_{\text{vol}}(J) + W_{\text{iso}}(\bar{I}_1, \bar{I}_2) + W_{\text{ani}}(\bar{I}_4, \bar{I}_5) + W_G(\bar{I}_{\alpha-6,7,8,9,10,11}), \tag{22}$$

where the free energy W_G is the energy contributed to the invariants $I_6 \sim I_{11}$ which is associated with the bending stiffness.

3. Determination of the Strain Energy Function and Corresponding Parameters of V-Belt

The V-belt shown in Figure 1 is a V-belt widely used in transmissions of automobiles, machines, and machine tools. It has a complicated structure and contains a fabric and a core wire in addition to rubber. The belt has anisotropic characteristics. Ishikawa et al. carried out a series of experiments and simulation studies [13]. The following is mainly based on the experimental data for the parameter fitting and simulation of the constitutive model.

3.1. Strain Energy and Parameters of Matrix Rubber. Matrix rubber is generally regarded as a hyperelastic material. In order to obtain accurate material parameters, the V-belt is subjected to transverse uniaxial tensile test. The stress-strain relationship can be approximated as the performance of the hyperelastic matrix rubber. Using the data fitting module of the ABAQUS hyperelastic part, considering the compressibility, Poisson's ratio of the rubber is set to 0.47. The typical Mooney–Rivlin model is used to compare the mechanical properties of the matrix material. The fitting curve is shown in Figure 2. The Mooney–Rivlin

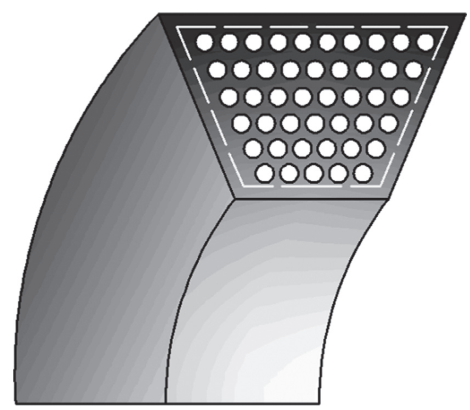

FIGURE 1: V-belt.

strain energy form of the rubber with compressibility is as follows:

$$W_{\text{iso+vol}} = \frac{1}{D}(J-1)^2 + C_{10}(\bar{I}_1 - 3) + C_{01}(\bar{I}_2 - 3). \tag{23}$$

The parameters obtained by fitting the transverse uniaxial stretching of the above curve are $D = 0.01763\,\text{MPa}^{-1}$, $C_{10} = -0.875\,\text{MPa}$, and $C_{01} = 4.3478\,\text{MPa}$,

3.2. Determination of the Strain Energy Form and Parameters of the Fiber Part. Tensile strain and fiber elongation have the following approximate relationship:

$$\varepsilon = \lambda - 1 = \sqrt{I_4} - 1, \tag{24}$$

where λ is the elongation of the fiber; we use equation (23) to obtain the relationship between stress and stress through the force-displacement curve and finally express the tensile

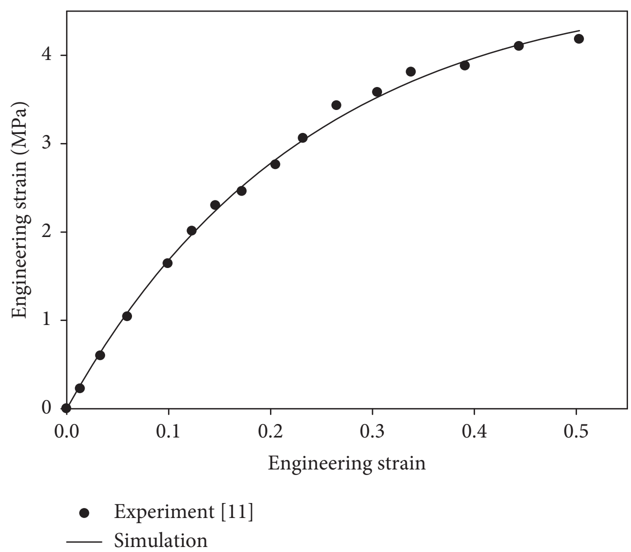

Figure 2: Stress-strain curve of uniaxial tensile of rubber.

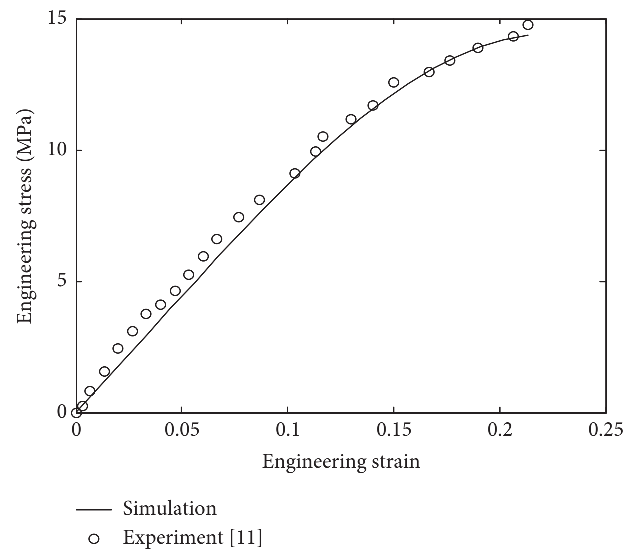

Figure 3: Stress-strain curve of fiber direction of longitudinally uniaxial tensile.

strain energy as a function $I_4 - 1$. The contribution of energy I_5 is related to the fiber-matrix interaction. It is written according to formula (6) as follows:

$$W_{\mathrm{ani}} = C_2\left(\bar{I}_4 - 1\right)^2 + C_3\left(\bar{I}_4 - 1\right)^4 + C_4\left(\bar{I}_5 - 1\right)^2 + C_5\left(\bar{I}_5 - 1\right)^4. \quad (25)$$

Data fitting was performed using MATLAB programming. The fitted curve is shown in Figure 3.

The final material parameters are $C_2 = 7.9718$, $C_3 = -6.7227$ MPa, $C_4 = 0.086$, and $C_5 = -0.027$ MPa. From the results of the above fitting, the free energy contributed by the invariant I_4 is much larger than the energy contributed by I_5. For a more detailed discussion, refer to Peng et al. [5].

3.3. Determination of Strain Energy and Parameters Contributed by Fiber Bending Stiffness. It can be seen from equation (13) that the invariants are all related to the curvature of the fiber. To simplify the formula, it is assumed that the deformation of the fiber is linear elastic, ignoring the term of the quadratic term and above, so that the strain energy contributing to the bending stiffness is only considered. I_9 which is in equation 20,

$$W_G = C_6\bar{I}_9^2. \quad (26)$$

Due to the influence of the bending stiffness, the generation of the couple stress and the stress matrix are no longer symmetrical, and MATLAB programming is used to solve the problem. Due to the lack of corresponding experimental data to determine the specific values C_6, separate energy function W_G is used to study the effect on bending deformation.

4. Numerical Simulation

Combining the material parameters obtained by the previous parameter, the corresponding finite element program is compiled to simulate the bending of the rubber-cord

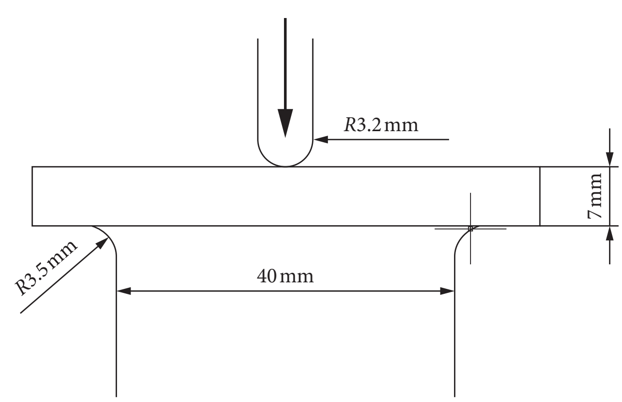

Figure 4: Schematic of numerical model.

composite, i.e., V-belt as shown in Figure 4. The cuboid sample of size 60 mm × 25 mm × 7 mm is cut from the V-belt, and the fiber direction is a group of longitudinal reinforcement.

Figure 5 shows the finite element model with a loading speed of 10 mm/min. Because of the symmetry of the model, we take half of the model to reduce the amount of calculation. As can be seen from Figure 5, when the lower portion of the sample is in a stretched state, the portion in contact with the indenter is in a compressed state. Figure 6 shows a graph of the mass force of the rigid indenter and the corresponding displacement. It can be seen that when the bending stiffness is zero, the curve obtained by the simulation is greatly different from the experimental curve, which also indicates the conventional continuous medium. The construction model is only fit for simple stretching and compression and is not fit for bending conditions. When C_6 is 5 MPa and 22.3 MPa, respectively, it can be seen that the curve obtained by the simulation and the curve of the experiment are gradually consistent. This proves the correctness of the hyperelastic constitutive model with bending stiffness.

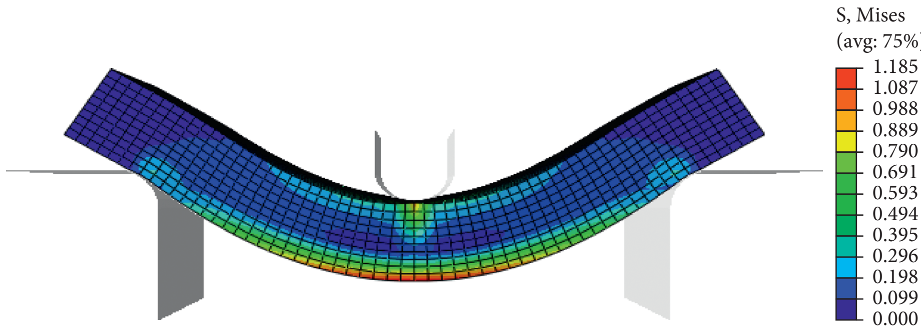

Figure 5: von Mises stress distribution of bending deformation.

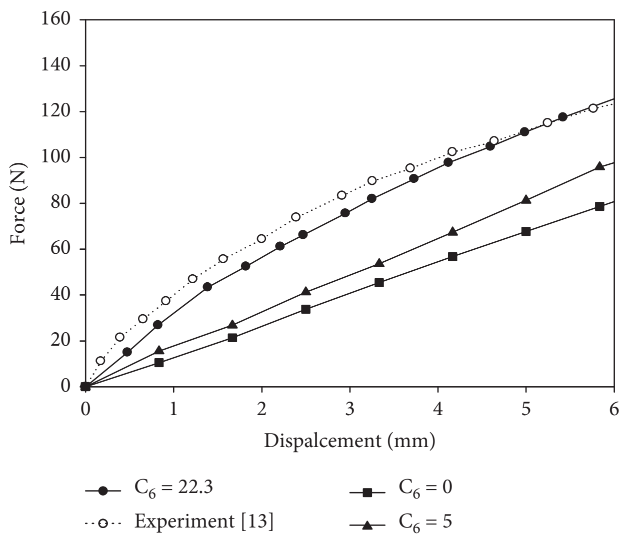

Figure 6: Force-displacement curve of bending test.

5. Conclusions

Both the theoretical and simulation results show that the constitutive model based on the conventional continuum mechanics has achieved great success, but it is only fit for the tensile or compression deformation and is not suitable for the bending deformation.

A set of parameter identification schemes was proposed. The parameters of matrix materials were fitted with the data by transverse uniaxial tensile test, and the parameters of the matrix were determined. Then, the uniaxial test along the cord direction is used to fit the other parameters of the constitutive equation, and finally all the material parameters of the constitutive equation except the bending stiffness are determined.

Based on the invariant theory of Spencer, we introduce the fiber vector and propose a new hyperelastic constitutive model with the interaction of bending stiffness for anisotropic fiber-reinforced belt. The results of experiments are in good agreement with the numerical simulations.

Data Availability

The data used to support the findings of this study are available from the corresponding author upon request.

Conflicts of Interest

The authors declare that they have no conflicts of interest.

Acknowledgments

This study was supported by the National Natural Science Foundation of China (11172171), the Science and Technology Project of Guizhou Province (no. 20161063), the Joint Fund of Guizhou Province (no. 20167105), and the Scientific Research Startup Project of High-Level Talent for GIT (XJGC20190928).

References

[1] J. Adkins and R. Rivlin, "Large elastic deformations of isotropic materials X. Reinforcement by inextensible cords," *Philosophical Transactions of the Royal Society of London Series A, Mathematical and Physical Sciences*, vol. 248, no. 944, pp. 201–223, 1955.

[2] A. J. M. Spencer, *Deformations of Fiber-Reinforced Materials*, Clarendon Press, Oxford, UK, 1972.

[3] A. J. M. Spencer and K. P. Soldatos, "Finite deformations of fibre-reinforced elastic solids with fibre bending stiffness," *International Journal of Non-linear Mechanics*, vol. 42, no. 2, pp. 355–368, 2007.

[4] T. H. Nam and B. Marvalová, "Deformation analysis of inflated cylindrical membrane of composite with rubber matrix reinforced by cords," in *Proceedings of the XXI International Congress of Theoretical and Applied Mechanics ICTAM 2004*, Warsaw, Poland, August 2004.

[5] X. Q. Peng, Z. Y. Guo, and B. Moran, "An anisotropic hyperelastic constitutive model with fiber-matrix shear interaction for the human annulus fibrosus," *Journal of Applied Mechanics*, vol. 73, no. 5, pp. 815–824, 2006.

[6] G. A. Holzapfel, T. C. Gasser, and R. W. Ogden, "A new constitutive framework for arterial wall mechanics and a comparative study of material models," *Journal of Elasticity and the Physical Science of Solids*, vol. 61, pp. 1–48, 2000.

[7] D. J. Steigmann, "Continuum theory for elastic sheets formed by inextensible crossed elasticae," *International Journal of Non-Linear Mechanics*, vol. 106, pp. 324–329, 2018.

[8] T. Asmanoglo and A. Menzel, "A multi-field finite element approach for the modelling of fiber-reinforced composites with fiber-bending stiffness," *Computer Methods in Applied Mechanics and Engineering*, vol. 317, pp. 1037–1067, 2017.

[9] T. Asmanoglo and A. Menzel, "Fiber-reinforced composites with fiber-bending stiffness under azimuthal shear–comparison

of simulation results with analytical solutions," *International Journal of Non-Linear Mechanics*, vol. 91, pp. 128–139, 2017.

[10] K. P. Soldatos, "On the characterisation of polar fibrous composites when fibers resist bending," *International Journal of Solids and Structures*, vol. 148-149, pp. 35–43, 2018.

[11] S. E. S. Bolouri, C. I. Kim, and S. Yang, "Linear theory for the mechanics of third-gradient continua reinforced with fibers resistance to flexure," *Mathematics and Mechanics of Solids*, vol. 25, no. 4, pp. 937–960, 2019.

[12] Q.-S. Zheng, "Theory of representations for tensor functions—a unified invariant approach to constitutive equations," *Applied Mechanics Reviews*, vol. 47, no. 11, pp. 545–587, 1994.

[13] S. Ishikawa, A. Tokuda, and H. Kotera, "Numerical simulation for fiber reinforced rubber," *Journal of Computational Science and Technology*, vol. 2, no. 4, pp. 587–596, 2008.